ISSN 1070-3632, Russian Journal of General Chemistry, 2015, Vol. 85, No. 5, pp. 1019–1024. © Pleiades Publishing, Ltd., 2015.
Original Russian Text © S.E. Kravchenko, A.G. Burlakova, Yu.M. Shulga, I.I. Korobov, I.A. Domashnev, N.N. Dremova, G.V. Kalinnikov, S.P. Shilkin, R.A. Andrievskii, 2015, published in Zhurnal Obshchei Khimii, 2015, Vol. 85, No. 5, pp. 720–725.

Special Features of Preparation of Nanosized Hafnium Diboride of Different Dispersity

S. E. Kravchenko, A. G. Burlakova, Yu. M. Shulga, I. I. Korobov, I. A. Domashnev, N. N. Dremova, G. V. Kalinnikov, S. P. Shilkin, and R. A. Andrievskii

Institute of Problems of Chemical Physics, Russian Academy of Sciences, pr. Semenova 1, Chernogolovka, Moscow oblast, 142432 Russia
e-mail: ssp@icp.ac.ru

Received December 8, 2014

Abstract—X-ray diffraction analysis, scanning electron microscopy, X-ray photoelectron spectroscopy, thermogravimetry, and elemental analysis have been applied to study the products of interaction of powder hafnium with fine-crystalline boron in the $Na_2B_4O_7$ ionic melt at 600–850°C and of $HfCl_4$ with $NaBH_4$ at 300–700°C.

Keywords: hafnium diboride, nanosized particle, ionic melt, sodium tetraborate, sodium borohydride, hafnium tetrachloride

DOI: 10.1134/S1070363215050023

Nanosized hafnium diboride is a typical nanosized boride of a group IV metal. Similarly to zirconium diboride, hafnium diboride can be prepared starting from the volatile borohydride decomposing upon heating following scheme (1) [1–5].

$$M(BH_4)_4 \xrightarrow{t} MB_2 + B_2H_6 + 5H_2 \ (M = Zr, Hf). \qquad (1)$$

Nanosized hafnium diboride can be also prepared via interaction of $HfCl_4$ with $NaBH_4$ at 600°C under inert [6, 7] or via high-temperature carbothermal reduction of a mixture of HfO_2 and B_2O_3 [8, 9].

We have earlier demonstrated the possibility of preparation of nanosized titanium and zirconium diborides upon interaction of titanium (zirconium) with boron in the $Na_2B_4O_7$ ionic melt [10–12]. Detailed study of this process is important in view of extending the knowledge on the influence of particles size on physico-chemical, mechanical, and other properties of various materials [13].

In this work we studied two routes to prepare nanosized HfB_2: via interaction of boron and hafnium powders in $Na_2B_4O_7$ ionic melt at 600–850°C (*a*) and via reaction of $HfCl_4$ with $NaBH_4$ at 300–700°C (*b*). In the latter case, in contrast to Ref. [6], initial heating of the reaction mixture was conducted in vacuum (0.133 Pa) rather than in an inert atmosphere.

Figures 1 and 2 and Table 1 show the conditions and the outcomes of interaction of equimolar amounts of powders of hafnium (0.83 g, 0.0046 mol) and boron (0.1 g, 0.0092 mol) in the presence of excess of $Na_2B_4O_7$ at 600–850°C. The results revealed that hafnium diboride was formed at ≥750°C, above the tetraborate melting point. The composition of hafnium diboride isolated from the reaction mixture (route *a*) as determined by chemical analysis and X-ray energy dispersive analysis was of $HfB_{2.02–2.03}$.

According to X-ray diffraction studies (Fig. 1), hafnium diboride formed crystals of hexagonal system, the lattice parameters being listed in Table 1; they well coincided with the reference data (a_0 = 0.3142 and c_0 = 0.3477 nm [14]).

Analysis of the diffraction peaks in the range of 2θ = 15°–110° using the Scherrer equation (2) revealed that the coherent scattering area of HfB_2 D_{hkl} was of ≈55 nm.

$$D_{hkl} = k\lambda/\beta_{hkl}\cos\theta_{hkl}. \qquad (2)$$

In Eq. (2), k stands for anisotropy parameter taken equal to 0.9, λ is the X-ray radiation wavelength [$\lambda(CuK_\alpha)$ = 1.54178 Å], θ is diffraction angle, and β is half-width of the diffraction peak (rad).

According to the scanning electron microscopy data, particles of the HfB_2 were of 50–55 nm (Fig. 2).

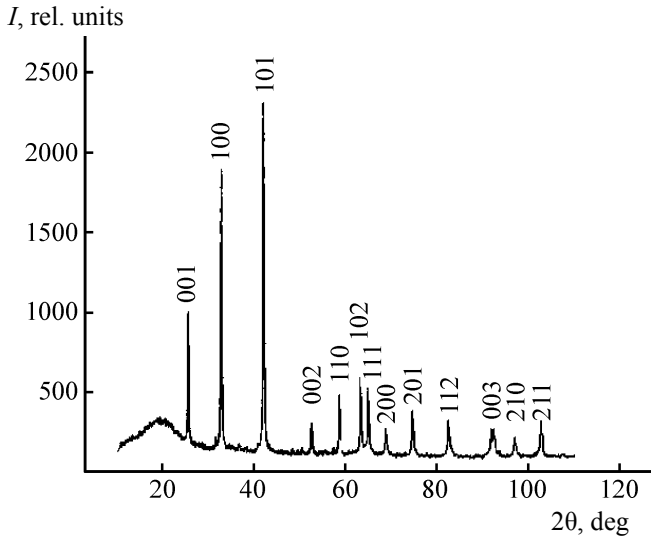

Fig. 1. X-ray diffraction pattern of HfB_2 powder prepared via interaction of boron and hafnium at 850°C in $Na_2B_4O_7$ ionic melt.

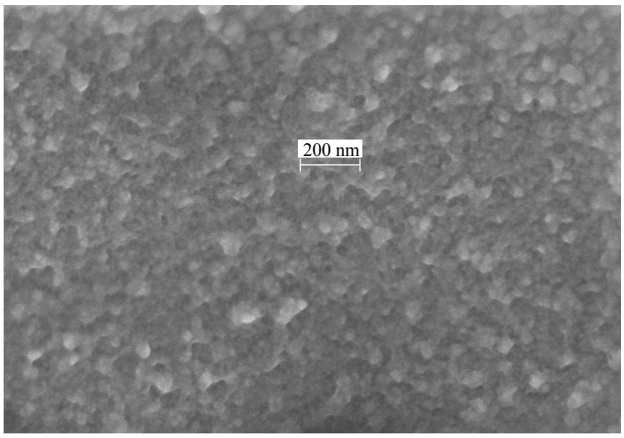

Fig. 2. Electron microscopy image of HfB_2 powder prepared via interaction of boron and hafnium at 850°C in $Na_2B_4O_7$ ionic melt.

The particles diameter calculated from the specific surface data under assumption of the spherical shape [S_{sp} = 9.3 m^2/g, $d(HfB_2)$ = 11.178 g/cm^3] was of ≈60 nm. Hence, the transfer of B to Hf in the $Na_2B_4O_7$ ionic melt could be explained by boron reduction to B^{2+} [Eq. (3)] followed by disproportionation to yield HfB_2 [Eq. (5)] [15].

$$B + 2B^{3+}_{melt} \rightarrow 3B^{2+}_{melt}, \quad (3)$$

$$3B^{2+}_{melt} + Hf \rightarrow B^{3+}_{melt} + HfB_2 + Q. \quad (4)$$

However, the proposed scheme of hafnium diboride formation in the $Na_2B_4O_7$ ionic melt should be further refined.

Table 2 shows the results of study of $HfCl_4$ (1.3 g, 0.0041 mol) interaction with excess of $NaBH_4$ (1 g, 0.027 mol) at 300–700°C. Formation of single-phase hafnium diboride occurred at $T \geq 550$°C, above decomposition temperature of $NaBH_4$ [16].

Chemical analysis and X-ray energy dispersive analysis revealed that hafnium diboride prepared at 550–700°C was of the $HfB_{2.02–2.04}$ composition, containing no chlorine admixture. X-ray diffraction study (Fig. 3) showed that hafnium diboride formed crystals of hexagonal system with the lattice parameters listed in Table 2; those values coincided well with the reference data [14].

Interaction of hafnium tetrachloride with excess of $NaBH_4$ at temperatures below 550°C yielded mixtures of hafnium diboride and an X-phase of unknown structure and composition (besides the three peaks assigned to HfB_2, two diffuse peaks were observed in the X-ray diffraction patterns; the lattice parameters were not determined due to the insufficient data).

Analysis of the diffraction peaks in the range of 2θ = 15°–110° using the Scherrer equation (2) revealed that the coherent scattering area of HfB_2 D_{hkl} was of

Table 1. Conditions and outcome of hafnium powder reaction with boron in $Na_2B_4O_7$ ionic melt

Chemical composition of the product	T, °C	Time, h	Phase composition of the product	Crystal lattice period, nm	
				a	c
$HfB_{2.02}$	600	15	Hf, B	–	–
$HfB_{2.03}$	750	15	HfB_2	0.3144	0.3481
$HfB_{2.03}$	800	10	HfB_2	0.3145	0.3472
$HfB_{2.02}$	850	10	HfB_2	0.3140	0.3480

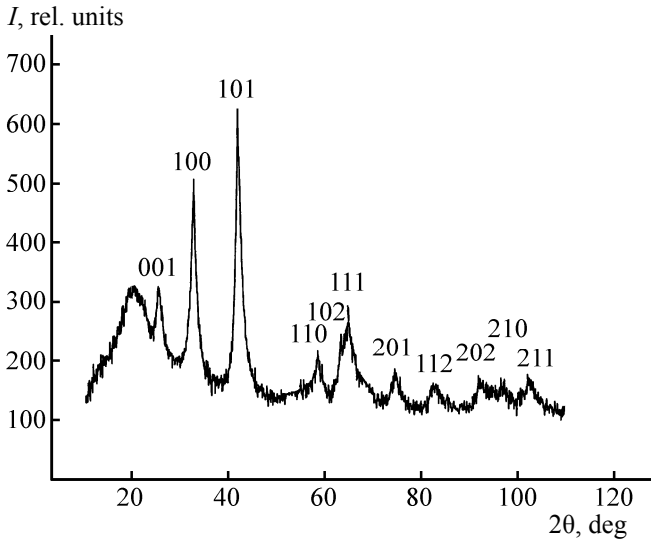

Fig. 3. X-ray diffraction pattern of HfB_2 powder prepared via interaction of $NaBH_4$ and $HfCl_4$ at 700°C.

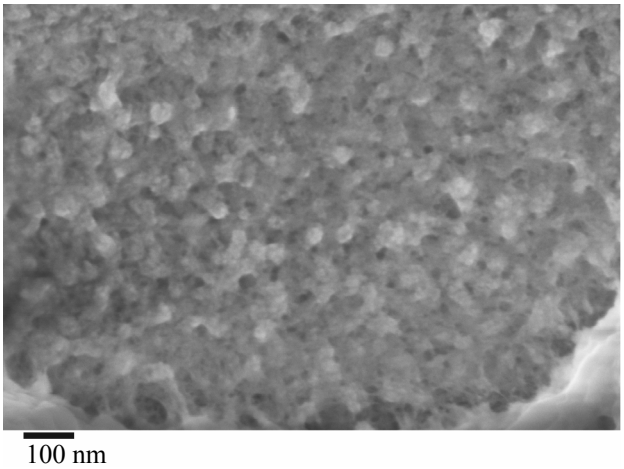

Fig. 4. Electron microscopy image of HfB_2 powder prepared via interaction of $NaBH_4$ and $HfCl_4$ at 700°C.

≈18 nm (the analysis was performed using the direction perpendicular to the *hkl* plane).

Amorphous part of HfB_2 gave rise to a broad halo at $10° \le 2\theta \le 25°$ with a maximum at ≈20° (the halo could partially appear due to the presence of the support).

Electron microscopy revealed that hafnium diboride powder prepared at 700°C consisted of the particles of different shape, part of them being close to spheres with diameter of 20–25 nm (Fig. 4); that was in accordance with the data on specific surface area (S_{sp} = 30.6 m^2/g) corresponding to equivalent particles diameter of ≈17 nm. Since the equivalent particles diameter determined from specific surface area was somewhat lower than the coherent scattering area, we concluded that amorphous part significantly contributed to specific surface area of the specimen.

Composition of surface of powder particles prepared via interaction of $HfCl_4$ with excess of $NaBH_4$ was refined using their X-ray photoelectron spectra. The $Hf4d_{5/2}$ line (Fig. 5) was a single asymmetric peak; the asymmetry was well described via the curve deconvolution into two Gaussian peaks. The fitting parameters are given in Table 3.

The stronger peak (*1*) was assigned to the presence of hafnium dioxide at the surface, whereas peak (*2*) corresponded to hafnium diboride [17]. Half-width of peak (*1*) was much higher than that of peak (*2*), pointing at the different nearest surrounding of hafnium atoms in the oxide layer. The oxide layer thickness *b* was estimated using Eq. (5):

$$A = I_{ox}/I_{met} = \exp(b/\Lambda_{ox}) - 1, \quad (5)$$

with I_{met}, integral intensity of $Hf4d_{5/2}$ line corresponding to hafnium in hafnium diboride; I_{ox}, integral intensity of the surface oxide line; and Λ_{ox}, free path of photoelectrons of $Hf4d_{5/2}$ in the oxide. According to the dependence of Λ on the photoelectron

Table 2. Conditions and outcome of the interaction of $NaBH_4$ with $HfCl_4$

Chemical composition of the product	*T*, °C	Time, h	Phase composition of the product	Crystal lattice period, nm	
				a	*c*
$Hf_{1.20}B_{2.45}H_{0.35}$	300	15	HfB_2 + X-phase	–	–
$Hf_{1.25}B_{2.30}H_{0.40}$	400	15	HfB_2 + X-phase	–	–
$HfB_{2.03}$	550	15	HfB_2	0.3146	0.3482
$HfB_{2.04}$	600	15	HfB_2	0.3138	0.3475
$HfB_{2.02}$	700	15	HfB_2	0.3140	0.3480

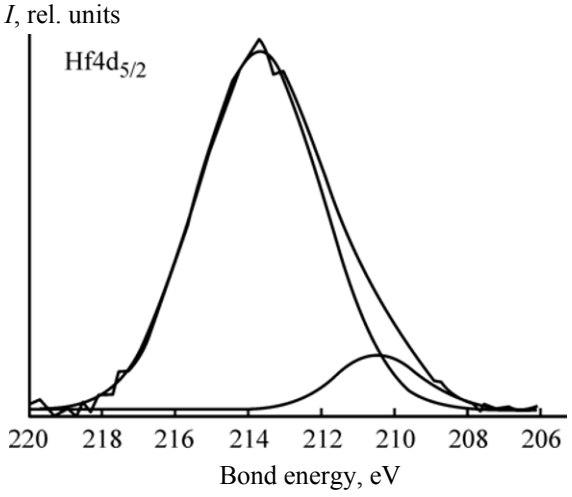

Fig. 5. X-ray photoelectron spectrum $Hf4d_{5/2}$ of HfB_2 powder prepared via interaction of $NaBH_4$ and $HfCl_4$ at 700°C.

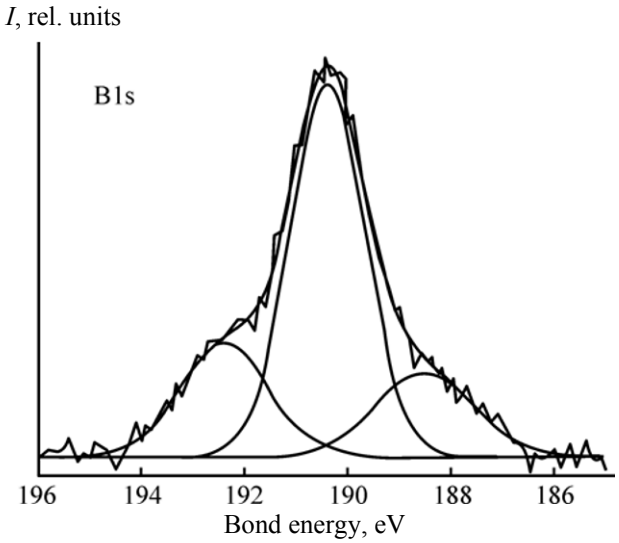

Fig. 6. X-ray photoelectron spectrum B1s of HfB_2 powder particles prepared via interaction of $NaBH_4$ and $HfCl_4$ at 700°C.

energy [18], in this work we took Λ equal to 1.0 nm. Accounting for the intensity values (Table 3), $b = 2.5$ nm.

The B1s spectrum contained three clearly revealed peaks (Fig. 6) with maximums at 192.4, 190.4, and 188.5 eV assigned to boron oxide (B_2O_3) or boric acid, hafnium boroxide (HfB_xO_y), and hafnium diboride, respectively [17, 19–21].

Hafnium diboride prepared via routes *a* and *b* did not change upon heating at 20–1000°C under argon atmosphere (no mass loss or heat evolution was detected). Surface composition of the prepared HfB_2 powders differed from that of bulk phase due to oxidation upon storage in air. Thickness of the oxidized layer was of ≈2.5 nm.

To conclude, preparation methods used in this work yield HfB_2 of different dispersity with the particles size of 20 to 60 nm. These methods allow fine tuning of the final product dispersity via altering the dispersity and chemical nature of the starting compounds.

Table 3. Parameters of $Hf4d_{5/2}$ spectrum fitting with two Gaussian functions

Peak no.	Deconvolution parameter (standard error)		
	position, eV	*I*, rel. units	half-width, eV
1	213.68 (0.03)	44720 (762)	3.49 (0.05)
2	210.36 (0.13)	4265 (649)	2.28 (0.18)

EXPERIMENTAL

Hafnium powder with 10–15 μm particles was prepared via activation of Hf (99.99%) filings by heating at 500°C in vacuum (0.13 Pa) followed by ten hydrogenation–dehydrogenation cycles. The hydrogenation was performed under hydrogen pressure of 5.0×10^6 Pa, and dehydration was carried out in vacuum (0.13 Pa) at 900°C as described elsewhere [22, 23]. Residual hydrogen and oxygen content in the powder was of 1.0×10^{-3}% and 3.0×10^{-3}%, respectively.

Hydrogen (99.999%) was supplied by autonomous laboratory hydrogen generator with the hydride phase based on the TiFe and $LaNi_5$ intermetallic compounds as working material [24, 25]. Commercially available boron ("pure" grade) with 10–20 μm particles was incubated in vacuum (0.13 Pa) at 300°C prior to the experiments. Anhydrous sodium borate was prepared via incubation of commercially available $Na_2B_4O_7 \cdot 5H_2O$ ("chemical pure" grade) in vacuum (0.13 Pa) at 350°C. Sodium borohydride (99.5%) was obtained via crystallization of the technical chemical from 1 M NaOH solution and dried in vacuum (0.133 Pa) at 100°C. Commercial hafnium tetrachloride (99.9%, 25–40 μm particles) was used as received.

X-ray diffraction studies were performed using an ADP-2 diffractometer (monochromatic CuK_α radiation). Accuracy of the lattice parameters determination was better than ±0.0003 nm.

Synchronous thermal analysis was performed using a Netzch STA 409 PC Luxx analyzer combined with a QMS403 C Aëolos quadrupole mass spectrometer (linear heating at 10 deg/min under argon stream, 20–1000°C).

Electron microscopy and X-ray energy dispersive analysis were performed using a measuring complex of a Zeiss Supra 25 scanning auto-emission electron microscope and an INCA x-sight X-ray spectral attachment. Electron microscopy pictures were obtained at low accelerating voltage (~4 keV), thus minimizing the contribution of the support into the measured signal.

X-ray photoelectron spectra were recorded using a Specs spectrometer upon excitation with MgK_α radiation ($h\nu$ = 1253.6 eV). Residual chamber pressure during the spectra recording was below 3×10^{-9} torr. The source power was of 225 W. The spectra were recorded in the constant transmission energy mode (30 eV in the case of the overview spectrum and 10 eV in the cases of the single lines). The data spacing was of 1 eV (overview) or 0.1 eV (single lines).

Specific surface area (S_{sp}) was determined from the low-temperature krypton adsorption after elimination of volatile admixtures at 1.33×10^{-3} Pa and 300°C; the calculations were performed using the Brunauer–Emmett–Teller method [25] taking the adsorbed krypton molecule area equal to 19.5×10^{-20} m^2. The relative accuracy of surface area and pores size distribution determination using a Quadrasorb SI analyzer was better than ±10%.

Boron content was determined by potentiometric titration of mannitol boronic acid with alkali after hafnium precipitation; hafnium was determined via complexometric titration in the presence of xylenol orange; chlorine was determined via turbidimetry or X-ray energy dispersive analysis.

Hydrogen and oxygen content in the metal phase was determined using a Vario Micro cube Elementar CHNS/O elemental analyzer.

Pressure was measured with a class 0.4 manometer.

Interaction of Hf, B, and $Na_2B_4O_7$. Equimolar amounts of Hf and B with excess of anhydrous $Na_2B_4O_7$ were mixed in a vibration mill (capacity 50 mL, ball loading 1 : 1, amplitude 10 mm, frequency 28 Hz) in argon atmosphere at room temperature during 8 h to get a fully homogenized mixture. The prepared mixture was put to a steel reactor (an autoclave, 30 mm in diameter and 200 mm long) in a corundum crucible. The reactor was evacuated to residual pressure of 0.13 Pa and heated at 600–850°C. The reactor was then cooled down to ambient, filled with argon, and the mixture was unloaded. The baked mixture was crushed, treated sequentially with distilled water, ethanol, and acetone, the ampoule was evacuated to residual pressure of 0.13·Pa and filled with argon.

Interaction of $HfCl_4$ with $NaBH_4$. Quartz ampoule with hafnium tetrachloride and excess of sodium borohydride was put to the reactor (steel autoclave) under high-purity argon atmosphere. The autoclave was evacuated at room temperature during 5 min and heated during 15 h at a predefined temperature. The reactor was then cooled to ambient, and the product was incubated in vacuum during 0.5 h. The product was unloaded under argon atmosphere, the reaction mass was treated sequentially with cooled distilled water, acetone, and ethanol, and incubated in vacuum (0.133 Pa) at 40°C during 5–6 h.

REFERENCES

1. Jensen, J.A., Gozum, J.E., Pollina, D.M., and Girolami, G.S., *J. Am. Chem. Soc.,* 1988, vol. 110, no. 5, p. 1643. DOI: 10.1021/ja00213a058.
2. Wayda, A.L., Schneemeyer, L.F., and Opila, R.L., *Appl. Phys. Lett.,* 1988, vol. 53, no. 5, p. 361. DOI: 10.1063/1.100603.
3. Andrievski, R.A., Kravchenko, S.E., and Shilkin, S.P., *Japan. J. Appl. Phys. Ser.,* 1994, vol. 10, p. 198.
4. Andrievskii, R.A., Kravchenko, S.E., and Shilkin, S.P., *Neorg. Mater*., 1995, vol. 31, no. 8, p. 1048.
5. Volkova, L.S., Torbov, V.I., and Shilkin, S.P., *Russ. J. Inorg. Chem.,* 2011, vol. 56, no. 4, p. 506. DOI: 10.1134/s0036023611040164.
6. Chen, L. Gu, Y., Chi, L., Shi, L., Yang, Z., Ma, J., and Qian, Y., *J. Alloys Compd.,* 2004, vol. 368, p. 353. DOI: 10.1016/j.jallcom.2003.08.086.
7. Wang, H., Lee, S.-H., and Kim, H.-D., *J. Am. Ceram. Soc.,* 2012, vol. 95, no. 5, p. 1493. DOI: 10.1111/j.1551-2916.2012.05141.x.
8. Carenco, S., Portehault, D., Boissiere, C., Mezailles, N., and Sanchez, C., *Chem. Rev.,* 2013, vol. 113, no. 10, p. 7981. DOI: 10.1021/cr400020d.
9. Venugopal, S., Paul, A., Vaidhyanathan, B., Binner, J.G.P., Heaton, A., and Brown, P.M., *Eur. Ceram. Soc.,* 2014, vol. 34, no. 6, p. 1471. DOI: 10.1016/j. jeureramsoc., 2013. 12.025.
10. Volkova, L.S., Shulga, Yu.M., and Shilkin, S.P., *Russ. J. Gen. Chem.,* 2012, vol. 82, no. 5, p. 819. DOI: 10.1134/s1070363212050027.

11. Volkova, L.S., Kravchenko, S.E., Korobov, I.I., Kolesnikova, A.M., Dremova, N.N., Burlakova, A.G., Kalinnikov, G.V., and Shilkin, S.P., *Inorg. Mater.,* 2013, vol. 49, no. 11, p. 1086. DOI: 10.1134/s0020168513110137.
12. Volkova, L.S., Kravchenko, S.E., Burlakova, A.G., and Shilkin, S.P., *Inorg. Mater*., 2013, vol. 49, no. 12, p. 1187. DOI: 10.1134/s0020168513120157.
13. Andrievskii, R.A., *Osnovy nanostrukturnogo materialovedeniya. Vozmozhnosti i problemy* (Fundamentals of Nanostructured Materials Science. Possibilities and Problems), Moscow: BINOM. Laboratoriya Znanii, 2012.
14. *Diagrammy sostoyaniya dvoinykh metallicheskikh sistem: Spravochnik* (The Phase Diagrams of Binary Metallic Systems: Handbook), Lyakishev, N.P., Ed., Moscow: Mashinostroenie, 1996, vol. 1.
15. Ilyushchenko, N.G., Anfinogenov, A.I., and Shurov, N.I., *Vzaimodeistvie metallov v ionnykh rasplavakh* (Interaction of Metals in Ionic Melts), Moscow: Nauka, 1991.
16. Dymova, T.N., Eliseeva, N.G., and Mikheeva, V.I., *Zh. Neorg. Khim*., 1967, vol. 12, no. 9, p. 2317.
17. Monticelli, C., Bellos, A., Zucch, F., and Dal Colle, M., *Electrochim. Acta*, 2007, vol. 52, p. 6943. DOI: 10.1016/j.electacta., 2007.05.014.
18. *Practical Surface Analysis. Auger and X-Ray Photoelectron Spectroscopy,* Briggs, D. and Seah, M.P., Eds., Chichester: John Wiley & Sons, 1990.
19. Aleshin, V.G., Kharlamov, A.N., and Chudinov, M.G., *Izv. Akad. Nauk SSSR, Ser. Neorg. Mater*., 1979, vol. 15, no. 4, p. 672.
20. Belyansky, M. and Trenary, M., *Chem. Mater*., 1997, vol. 9, p. 403. DOI: 10.1021/cm9604423.
21. Perkins, C.L., Singh, R., Trenar, M., Tanaka, T., and Paderno, Yu., *Surface Sci*., 2001, vol. 470, p. 215. DOI: 10.1016/s0039-6028(00)00862-1.
22. Semenenko, K.N., Shilkin, S.P., Burnasheva, V.V., Korobov, I.I., and Volkova, L.S., *Zh. Obshch. Khim.*, 1983, vol. 53, no. 5, p. 961.
23. Semenenko, K.N., Shilkin, S.P., Burnasheva, V.V., Volkova, L.S., and Mozgina, N.G., *Zh. Obshch. Khim.*, 1987, vol. 57, no. 4, p. 729.
24. Semenenko, K.N., Shilkin, S.P., Burnasheva, V.V., Volkova, L.S., and Govorkova, L.V., Mozgina N.G., *Zh. Obshch. Khim*., 1984, vol. 54, no. 3, p. 491.
25. *Eksperimental'nye metody v adsorbtsii i molekulyarnoi khromatografii* (Experimental Methods in Molecular Adsorption Chromatography), Kisilev, A.V. and Dreving, V.P., Eds., Moscow: MGU, 1973.